Sjöberg, B.-M., Hahne, S., Mathews, C. Z., Mathews, C. K., Rand, K., & Gait, M. J. (1986a) *EMBO J. 5*, 2031–2036.
Sjöberg, B.-M., Sanders-Loehr, J., & Loehr, T. M. (1986b) *Biochemistry* (submitted for publication).
Slichter, C. P. (1963) *Principles of Magnetic Resonance*, p 155, Harper & Row, New York.
Thelander, L., & Reichard, P. (1979) *Annu. Rev. Biochem. 48*, 133–158.
Thelander, L., & Gräslund, A. (1983) *J. Biol. Chem. 258*, 4063–4066.
Thelander, L., & Berg, P. (1986) *Mol. Cell. Biol.* (in press).
Thelander, L., Eriksson, S., & Åkerman, M. (1980) *J. Biol. Chem. 255*, 7426–7432.
Thelander, L., Gräslund, A., & Thelander, M. (1983) *Biochem. Biophys. Res. Commun. 110*, 859–865.
Thelander, M., Gräslund, A., & Thelander, L. (1985) *J. Biol. Chem. 260*, 2737–2741.
Tsibris, J. C. M., Tsai, R. L., Gunsalus, I. C., Orme-Johnson, W. H., Hansen, R. E., & Beinert, H. (1968) *Proc. Natl. Acad. Sci. U.S.A. 59*, 959–965.
Wertz, J. E., & Bolton, J. R. (1972) *Electron Spin Resonance*, p 464, McGraw-Hill, New York.

Reversible Unfolding of Ribosomal Protein E-L30: An NMR Study†

F. J. M. van de Ven and C. W. Hilbers*
Laboratory of Biophysical Chemistry, University of Nijmegen, Toernooiveld, 6525 ED Nijmegen, The Netherlands
Received November 19, 1986; Revised Manuscript Received April 16, 1987

ABSTRACT: Ribosomal protein E-L30 unfolds reversibly at pH values between 7.0 and 4.5. Unfolding of the protein involves a fast and a slow equilibrium, which depend on the degree of protonation of His_{19} and His_{33}. Both the fast equilibrium between protonated and deprotonated histidines and the slow equilibrium between folded and unfolded protein could be monitored by means of 500-MHz ^1H NMR spectroscopy. The degree of protonation of His_{19} and His_{33} appears to be determinant in the unfolding process of the protein. It is shown however that even when the histidines are uncharged, the protein has only limited stability, probably as a result of the presence of all four Glu's of E-L30 in its triple-stranded β-sheet. At equimolar concentrations of the folded and unfolded form, the rate constant characterizing the transition between these forms is approximately 0.14 s^{-1}. Making use of sequential resonance assignments of the ^1H NMR spectrum [van de Ven, F. J. M., & Hilbers, C. W. (1986) *J. Mol. Biol. 192*, 419–441], the fast equilibrium could be interpreted in terms of alterations in the spatial structure of E-L30 in a specific domain of the molecule. This domain is also affected by temperature although not in exactly the same manner as by pH.

Now that the determination of primary structures of all proteins of the *Escherichia coli* ribosome has been completed (Wittmann, 1982), attention is focusing on the elucidation of the three-dimensional structures of ribosomal proteins (Leyonmarck et al., 1980; Littlechild et al., 1979; Kime et al., 1981; Gudkov et al., 1982; Giri et al., 1979; Appelt et al., 1981, 1983; van de Ven et al., 1983, 1984). The first determination of a spatial structure of a ribosomal component, by means of X-ray crystallography, concerned the C-terminal fragment of protein E-L7/L12 (Leyonmarck et al., 1980). Recently, the spatial structure of the first intact ribosomal protein was successfully investigated by means of X-ray crystallography as well as by NMR. In our laboratory we set out to study the protein E-L30 from the large subunit of the *E. coli* ribosome by means of two-dimensional fourier transform nuclear magnetic resonance (2D FT NMR) (van de Ven et al., 1984; van de Ven & Hilbers, 1986a,b) thereby using strategies mainly developed by K. Wüthrich and collaborators (Nagayama & Wüthrich, 1980; Wagner et al., 1980; Wüthrich et al., 1982; Billiter et al., 1982; Williamson et al., 1984). As a result, we succeeded in obtaining sufficient sequential ^1H NMR resonance assignments and nuclear Overhauser enhancement (NOE) data to present a model for the three-dimensional structure of E-L30 in solution (van de Ven & Hilbers, 1986a,b).

The application of X-ray crystallography for the elucidation of the structures of ribosomal proteins of *E. coli* has been hampered by difficulties in obtaining good crystals (Appelt et al., 1981). However, crystallization has been more successful for ribosomal proteins from *Bacillus stearothermophilus*, and the first structure obtained for these proteins is that of B-L30 of *B. stearothermophilus* (K. S. Wilson, K. Appelt, J. Dijk, I. Tanaka, and S. W. White, personal communication). The proteins E-L30 and B-L30 are 53% homologous (Kimura, 1984), and it was found that the crystal structure of B-L30 and the solution structure of E-L30 are much alike. Moreover, both these proteins appear to be remarkably similar to the C-terminal domain of E-L7/L12 (Leyonmarck et al., 1980) in that they consist of two layers: one layer composed of a triple-stranded antiparallel β-sheet, and one layer composed of two or three antiparallel α-helices.

A major advantage of the application of NMR in protein structural studies is that the folding of these macromolecules can be studied as a dynamic entity (Jardetzky, 1981). Thus, information may be obtained about "ring flipping" of aromatic residues (Campbell et al., 1977), about exchange rates of peptide bond amide protons (Glickson et al., 1969; Wagner & Wüthrich, 1979), about conformational changes relating to biological function (Moonen & Müller, 1984; Ogawa & Shulman, 1972), and about rates and mechanisms of protein folding. In this paper it will be shown that in solution E-L30 is a dynamic system involving multiple forms of the protein in mutual equilibria. The degree of protonation of both histidines in E-L30, His_{19} and His_{33}, appears to be a vital parameter in the equilibrium between folded and unfolded forms of E-L30. A model, which describes the observed phenomena, will be presented.

† This research was supported by the Netherlands Foundation for Chemical Research (SON) with financial aid from the Netherlands Organization for the Advancement of Pure Research (ZWO).

0006-2960/87/0426-5548$01.50/0

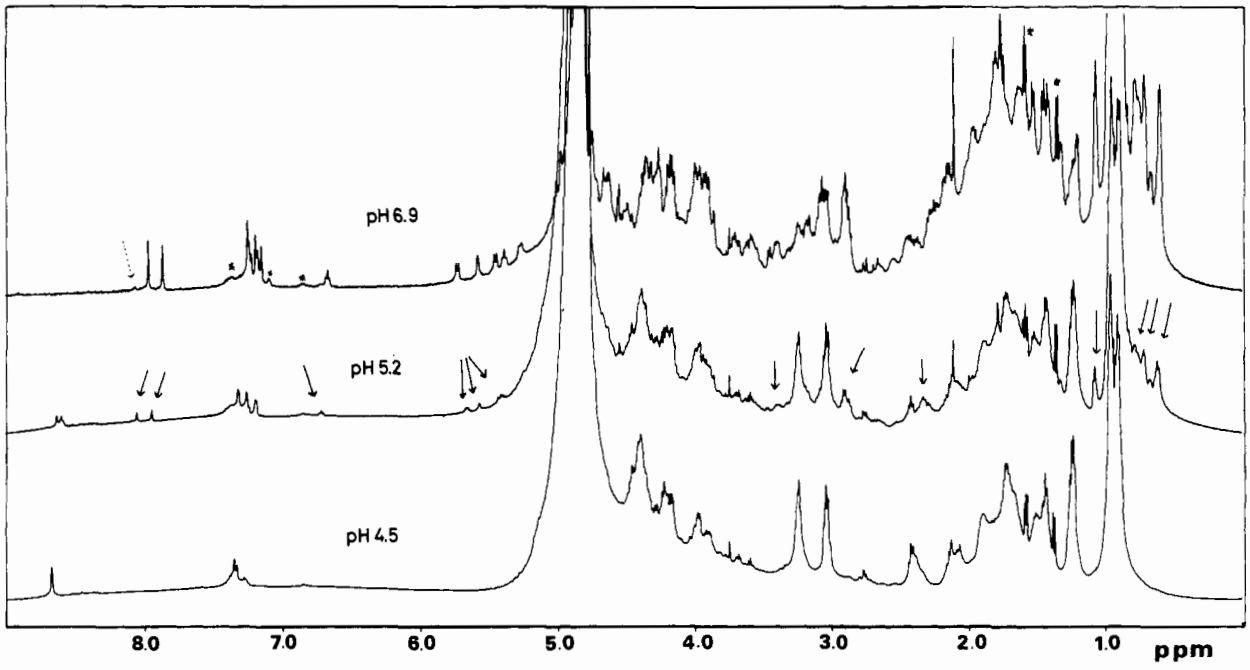

FIGURE 1: The 500-MHz ^1H NMR spectra of E-L30 recorded at 297 K and at three different pH values. The spectrum obtained at pH 4.5 corresponds to that of the unfolded protein; the spectrum obtained at pH 6.9 corresponds to the folded protein. The dotted arrow points at a signal belonging to 5% irreversibly denatured protein. The middle spectrum, recorded at pH 5.2, is a 1/1 mixture of the spectra of the folded and unfolded protein. The arrows in this spectrum point at resonances originating from folded protein. The asterisks indicate impurities.

Materials and Methods

Protein E-L30 was isolated from *E. coli* MRE 600 essentially as described earlier (van de Ven et al., 1983): ribosomal proteins were fractionated by column chromatography on phosphocellulose, and E-L30 was subsequently purified by gel filtration. The buffers used in the isolation procedure contained 6 M urea, causing denaturation of the proteins. E-L30 was renatured by dialysis of a solution of the protein in 6 M urea against a buffer containing 20 mM potassium phosphate, 0.1 M KCl, and 0.02% sodium azide at pH 6.85 (van de Ven et al., 1983). This buffer was also used for the preparation of NMR samples, which contained 0.5–1.0 mM E-L30 and 99.8% D_2O (Aldrich).

Spectra were recorded at different pH values and temperatures on a Bruker WM 500 spectrometer operating in the Fourier transform mode at 500 MHz. Usually about 500 transients were accumulated. Observation pulses with flip angles of 45° and relaxation delays of 4 s (including acquisition times of 1 s) were used to ensure complete relaxation of spins of both folded and unfolded protein.

pH values (pH meter readings) of the NMR samples were adjusted by addition of small amounts of dilute NaOD or DCl (Aldrich). pH was checked before and after recording of ^1H NMR spectra and was found to be constant to within 0.05 unit.

As an internal reference for temperature calibration (Hartel et al., 1982), tetramethylammonium chloride was added to a concentration of about 1 mM. Chemical shifts are quoted relative to 3-(trimethylsilyl)[2,2,3,3-$^2H_4$]propionate at neutral pH.

Results and Discussion

pH Dependence. In earlier experiments, related to the elucidation of the structure of E-L30, we had noticed that the protein can be reversibly denatured as a function of pH between pH values of 7.0 and 4.5. The main candidates for protonation and deprotonation in this pH region are the histidyl imidazole groups. According to the spatial structure of the protein, histidines His_{19} and His_{33} are located in the hydrophobic interior of the E-L30 molecule, together with the only other aromatic amino acid: Phe_{52}. Also, the NMR data indicate that the N1 atom of His_{33} is involved in a hydrogen bond with the amide proton of Arg_{29} (van de Ven & Hilbers, 1986b). To assess whether His_{19} and/or His_{33} in E-L30 exhibits normal or anomalous titration behavior, spectra were recorded at different pH values; three typical spectra obtained in this series are shown in Figure 1. The bottom spectrum, which was recorded at pH 4.5, is typical for a randomly coiled protein. The spectrum can be simulated by adding up the separate spectra of the different amino acids that are present in E-L30. Thus, all resonances of the methyl protons of valines, leucines, and isoleucines are crowded in one peak at about 0.95 ppm, all six threonine $C^\delta H_3$ protons resonate at about 1.25 ppm, five lysine $C^\epsilon H_2$ and six arginine $C^\delta H_2$ resonances are found at 3.0 and 3.3 ppm, respectively, and both histidine C2H resonances coincide at 8.64 ppm, indicating complete protonation of their imidazole groups.

When a small amount of dilute NaOD is added to raise the pH to 5.2, many new peaks appear in the spectrum indicated by arrows in Figure 1. Upfield from 0.8 ppm several resonances appear, and also in the aromatic region of the spectrum new peaks make their entry, e.g., a triplet at 6.72 ppm. These are typical features of the folding of a protein: aromatic rings and methyl groups forming hydrophobic domains. The aromatic rings give rise to ring-current shifts on the CH_3 resonances, and perturbations occur in the spectra of aromatic ring protons. Also, in other spectral regions new peak appear, e.g., at 1.05 ppm, at 2.35 ppm, and downfield from 5.00 ppm. The latter resonances are typical of $C^\alpha H$ protons in the interior of β-sheets (Pardi et al., 1983). Numerous changes are also occurring in the more crowded spectral region between 2.5 and 4.5 ppm, giving rise to a generally more dispersed spectrum.

Simultaneously with the appearance of many new resonances, several of the others are disappearing; i.e., the bulk threonine $C_\gamma H_3$ resonance at 1.25 ppm is clearly diminishing. Since resonances disappear from crowded regions and often reappear in sparsely populated spectral regions, the appearance of new resonances is easier to assess than the disappearance of old ones. A favorable exception is formed by the C2H

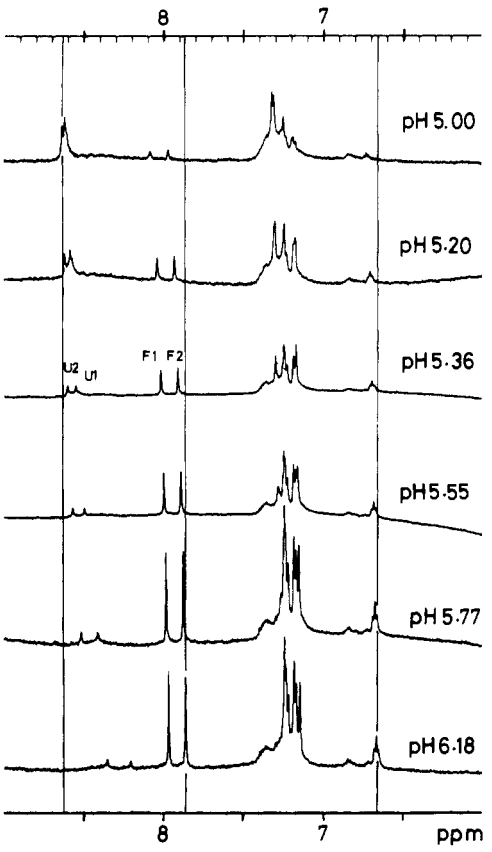

FIGURE 2: pH dependence of the aromatic region of the 500-MHz ^{1}H NMR spectrum of E-L30. The pH values at which the spectra were recorded are shown on the right. Vertical lines are drawn to emphasize the pH-dependent shifting of resonances. Resonances U1 and U2 originate from the histidine C2H protons of unfolded protein, and resonances F1 and F2 originate from the same protons of folded protein (see spectrum recorded at pH 5.36).

resonances of the histidines in the extreme low-field part of the spectrum. Here it is clearly seen that the disappearing spectrum, contributing two resonances at 8.60 and 8.57 ppm, and the appearing spectrum, contributing C2H resonances at 8.04 and 7.94 ppm, are of approximately equal intensity. This means that, as far as histidines are concerned, refolding of E-L30 is about halfway complete at pH 5.2.

The top spectrum of Figure 1 was recorded at pH 6.9. It is clearly seen that the trends in spectral changes observed in going from pH 4.5 to pH 5.2 persist when the pH is raised further. In the low-field part of the spectrum a tiny peak originating from a C2H proton of a random coil histidine is still visible at 8.05 ppm. Judging from its intensity, relative to that of both resonances of histidines belonging to "folded" protein, renaturation is almost complete at pH 6.9.

From the data presented in Figure 1 it is concluded that at pH values between 4.5 and 7.0 a folded and an unfolded form of E-L30 are in equilibrium. Transfer between the two forms is slow on the NMR time scale. Lowering the pH causes unfolding, and raising the pH causes folding. It is noted in passing that during recording of the "pH dependence" spectra we found that the equilibrium is established within a few minutes: the time it took to adjust the pH and record a spectrum. Spectra recorded after 1 h were identical with those recorded directly after pH adjustment.

For a more quantitative analysis of the equilibrium between folded and unfolded protein on the one hand and between protonated and deprotonated histidines on the other hand, we concentrate on the downfield resonances shown in Figure 2 for a number of pH values. The resonances of C2H protons

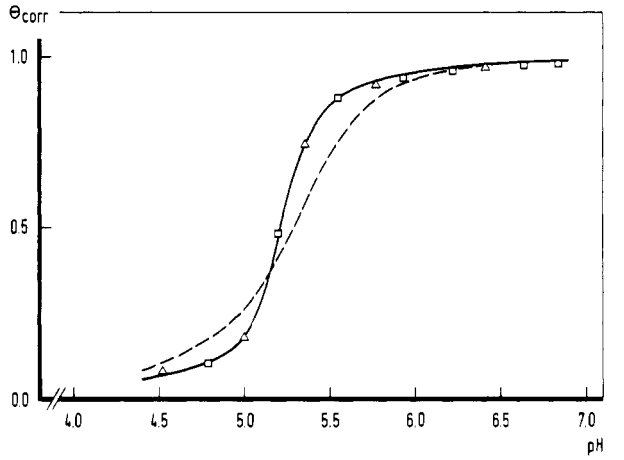

FIGURE 3: Fraction of folded E-L30 protein measured as a function of pH at 297 K. The fraction of folded protein was calculated from the relative intensities of the U and F resonances and corrected for the presence of irreversibly denatured protein as described in the text. Squares represent θ values obtained while raising the pH from 4.5 to 7; triangles represent θ values obtained while lowering the pH from 7 to 4.5. The dashed curve was calculated for a model in which only pK differences for histidines in folded and unfolded protein were taken into account (see text). The drawn line was calculated for a model in which pK differences for histidines as well as glutamates and aspartates are present (see text).

of histidines are used to determine the fraction of folded protein (θ) as a function of pH according to

$$\theta = i_f/(i_f + i_u) \quad (1)$$

Here, i_f and i_u are the sums of intensities of both resonances originating from "folded" (labeled "F") and "unfolded" (labeled "U") histidines.

The analysis of the data is hampered by the fact that our samples contain some irreversibly denatured material, varying from one preparation to another, usually amounting to some 5%. Irreversible denaturation may be caused by hydrolysis of side-chain amide groups of Asn_{48} and Gln_8. [The latter may well play an important role with respect to the stability of the protein (van de Ven & Hilbers, 1986b).] Hydrolysis of Asn and Gln side chains has been noted to occur during NMR studies of other proteins as well, e.g., trypsin-inhibitors like BPTI (Richarz et al., 1979) and BUSI IIA (Strop et al., 1983). Also, it is noted that during our isolation procedure for E-L30, which takes about 2 months in all, the protein is dissolved in 6 M urea (van de Ven et al., 1983). It is not unlikely that during this period some cyanate and other products of urea isomerization or cleavage are generated that may react with primary amino groups of the protein (White, 1967; Stark, 1967; Wystop et al., 1979), thereby causing irreversible denaturation. The data in Figure 3 have been corrected for the presence of 5% irreversibly denaturated protein as follows: $\theta_{cor} = \theta/0.95$, with θ given by eq 1.

In Figure 3, θ_{cor} is plotted against pH; it is seen that the folding–unfolding equilibrium is reversible; i.e., the renaturation and denaturation curves coincide.

Figure 2 shows that the resonance positions of the C2H protons of both forms are pH dependent. The pH dependence of the chemical shifts of C2H resonances is essentially as expected for histidines (Bundi & Wüthrich, 1979; Sudmeier et al., 1980): they resonate at about 8.65 ppm at low pH and upfield from 8 ppm at high pH. This shifting reflects the fast chemical exchange between protonated and deprotonated imidazole rings of histidines.

In Figure 4 the chemical shifts of all C2H resonances have been plotted against pH. Assuming fast chemical exchange

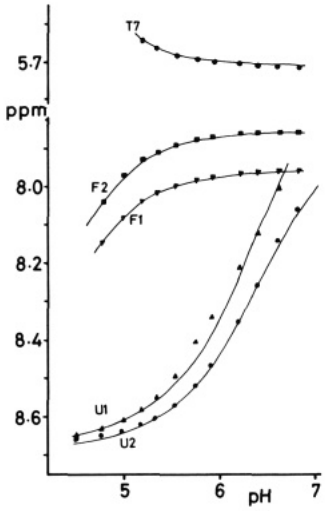

FIGURE 4: pH dependence of the chemical shifts of the C2H protons of the histidines in folded E-L30 protein (F1 and F2) and in unfolded protein (U1 and U2). The complete curves could not be obtained because the F resonances disappear at low pH and the U resonances at high pH. Also shown (top) is the pH-dependent chemical shift of the $C^{\alpha}H$ resonance of Thr_7. The lines through the data points represent the best fits obtained by taking $pK_u = 6.4$ and $pK_f = 4.3$ (see text).

between two sites, i.e., protonated histidine with chemical shifts δ_a and deprotonated histidine characterized by chemical shift δ_b, the degree of dissociation (α) may be derived from the observed chemical shifts, δ_{obsd}, according to

$$\alpha = (\delta_{obsd} - \delta_a)/(\delta_b - \delta_a) \quad (2)$$

Assuming independent protonation sites, a pK value may be derived from the data according to

$$pH = pK + \log [(\delta_{obsd} - \delta_a)/(\delta_b - \delta_{obsd})] \quad (3)$$

It was only possible to make estimations for δ_b of both "U" resonances and for δ_a of both "F" resonances; the "U" peaks become vanishingly small at high pH, and the "F" resonances disappear completely at low pH. Nevertheless, by curve fitting reasonable estimates of pK_u and pK_f are obtained (vide infra).

In addition to the histidines, several other residues in the folded form of E-L30 give rise to pH-dependent chemical shifts of their resonances, e.g., the ζ ring proton of Phe_{52} and the downfield-shifted $C_{\alpha}H$ resonances of Thr_7 and Thr_{34} (Figure 5). The chemical shift vs. pH curve for Thr_7 $C_{\alpha}H$ has been included in Figure 4. Residues Thr_7, His_{19}, His_{33}, Thr_{34}, and Phe_{52} are all located on the same side of the E-L30 molecule, and it is likely that shifting the Thr_7 and Thr_{34} resonances reflects titration of His_{33} and that shifting of the Phe_{52} $C_{\zeta}H$ resonance is caused by titration of His_{19}. In Figure 6 the positions of these five residues in our proposed model of E-L30 (van de Ven & Hilbers, 1986b) have been indicated.

A model that describes the pH-dependent behavior of E-L30 should simultaneously account for the fast-exchange titration curves of Figure 4 and the slow-exchange renaturation curve of Figure 3. In a "realistic" description of pH-induced protein denaturation, there are several aspects to consider (Tanford, 1968; Matthew et al., 1985): First, it may be that a two-state model featuring only completely folded and completely unfolded protein is too crude and that there exist intermediate states. However, for a small protein of the size of E-L30 an "all or none" model should be adequate. Second, different residues of a given amino acid type may have different pK's in the folded form of the protein. In the unfolded form, one would expect their pK's to be more similar. Third, cooperative effects are to be considered, both with respect to titration

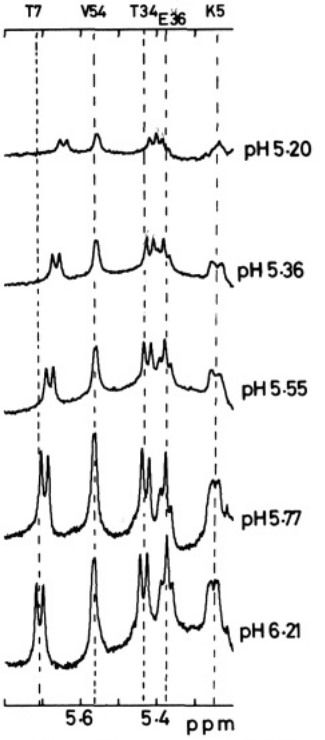

FIGURE 5: pH dependence of resonances of $C^{\alpha}H$ protons situated in the interior of the triple-stranded β-sheet of E-L30. The assignment of the resonances (van de Ven & Hilbers, 1986a,b) is indicated at the top. The dashed vertical lines are drawn to mark the positions of the resonances at neutral pH.

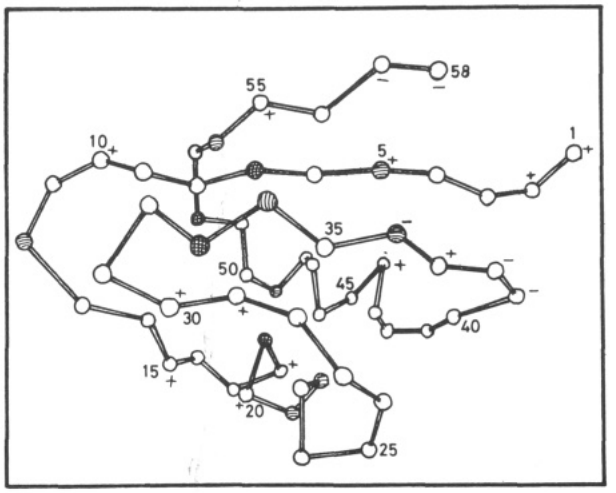

FIGURE 6: Three-dimensional structure of protein E-L30 derived from two-dimensional NMR studies (van de Ven & Hilbers, 1986a,b). Only the positions of the C^{α} atoms are shown. The residues with pH-dependent (circle with vertical lines), temperature-dependent (circles with horizontal lines), or both pH- and temperature-dependent (circles with crossed lines) resonances are indicated. Positively and negatively charged sites are marked (+) and (−), respectively.

behavior, i.e., the effective pK of a group being dependent on the (proton) charge density of its environment, and with respect to unfolding, i.e., partial unfolding triggering the complete denaturation of the molecule.

In this paper we will not attempt to create a model that fully complies with the complications of pH-induced protein unfolding. To test the quantitative aspects of such a model would require much more information than presently available. Rather, we seek to find out whether it is just the histidines that have different pK's in folded and unfolded E-L30 or if other residues are also of importance. The simplest model achieving this merely assumes a (slow) equilibrium between

two states: folded (F) and unfolded (U) protein. The pH dependence of this equilibrium is then caused by the fact that certain groups (here histidines) have different pK's in U and F. The situation is slightly complicated because there are more than one of such titratable groups in the protein molecule. The easiest way to deal with this problem is to assume that they are identical and independent. Then, if there are n groups with pK_u in the U form and pK_f in the F form of the protein and if the equilibrium constant between deprotonated U and F is $K_r = [F]/[U]$, the following expression is valid for θ, the fraction of folded protein:

$$\frac{\theta}{1-\theta} = \frac{K_r(1 + [H^+]/K_f)^n}{(1 + [H^+]/K_u)^n} \quad (4)$$

If we only take the histidines into account we have $n = 2$. Since the actual transition in Figure 3 takes place at pH values for which pH > pK_f, our, discutable, assumption regarding independent titration of histidines in the F form has little bearing on the quantitative evaluation: for the greater part of the curve we have that $[H^+]/k_f < 1$ and

$$\frac{\theta}{1-\theta} \simeq \frac{K_R}{(1 + [H^+]/K_n)^n} \quad (4a)$$

Hence, the data are not very discriminative for the exact details of titrations of histidines in the F form. Assuming both histidines to have identical pK's seems reasonable with respect to the titration curves shown in Figure 4.

The steepest relation between θ and pH would be obtained if there is maximum cooperativity. Then there are only two relevant species, protonated U and deprotonated F:

$$H_1U \rightleftarrows F + 2H^+$$

Then we have that

$$\frac{\theta}{1-\theta} = K_r\left(\frac{K_u}{[H^+]}\right)^2 \text{ and } \left[\frac{\text{d log}\left(\frac{\theta}{1-\theta}\right)}{\text{d pH}}\right]_{max} = 2 \quad (5)$$

In addition to the histidines, also the pK's of glutamates and aspartates may be different in folded and unfolded protein. One reason for such a pK difference can be that in the folded form these negatively charged side chains interact with positively charged ones, resulting in a lower apparent pK_a ("reluctance" to give up the negative charge by protonation). Actually, in E-L30 all glutamates and aspartates are involved in such interactions. All four glutamates are present in a triple-stranded β-sheet (van de Ven & Hilbers, 1986a,b; K. S. Wilson, K. Appelt, J. Dijk, I. Tanaka, and S. W. White, personal communication). Each of these glutamates can form an ion pair with a positively charged residue, i.e., Glu_{36}–Lys_5, Glu_{38}–Arg_{37}, Glu_{57}–Lys_{55}, and Glu_{58}–Arg_{44}. Also, the single aspartate in E-L30, Asp_{39}, can form an ion pair with Lys_2, the terminal NH_3^+ group, or both.

If we assume, for the sake of simplicity, that the four glutamates and the one aspartate together constitute a set of five independent and identical sites with pK_n in the folded form and pK_c in the unfolded form, then we have that

$$\frac{\theta}{1-\theta} = \frac{K_r(1 + [H^+]/K_f)^2}{(1 + [H^+]/K_u)^2} \frac{(1 + [H^+]/K_n)^5}{(1 + [H^+]/K_c)^5} \quad (6)$$

The values of K_f and K_u are derived from the data in Figure 4. We find that pK_u = 6.4 ($K_u = 4 \times 10^{-7}$) and pK_f = 4.3 ($K_f = 5 \times 10^{-5}$) give the best fits. The drawn lines in Figure 4 represent theoretical curves computed with eq 2 and 3. The parameters K_r, K_n, and K_c are determined by fitting eq 6 to the data of Figure 3.

If we disregard the five acidic side chains and only account for the two histidines, we use eq 4, which means that we basically have a one-parameter (K_r) model. The best fit through the experimental points is obtained by setting K_r = 250. The resulting curve, calculated with eq 4, is shown as a broken line in Figure 3. It is apparent that eq 4 cannot fully account for the actually observed data. Evidently there is a steeper relation between θ and pH than the model accounts for. For the steepest part of Figure 3 we have that

$$\frac{\text{d log } [\theta/(1-\theta)]}{\text{d pH}} \simeq 3$$

Hence, a model with only two protonation sites could never properly explain the data. The drawn line in Figure 3 represents the pH dependence of θ calculated with eq 6. The curve goes through all data points if in addition to the earlier established values pK_u = 6.4 and pK_f = 4.3 we set pK_n = 2, pK_c = 5.5, and K_r = 600. The parameters pK_u = 6.4 and pK_c = 4.5 represent typical "random coil pK values" of histidines and glutamates (Cantor & Schimmel, 1980; Matthew et al., 1985), and the decrease of about 2 units for the pK's of these residues in the folded form is quite reasonable with respect to the relative stabilities of hydrophobic and/or ionic interactions. These pK differences alone do not imply that E-L30 will denature below pH 6; this is a consequence of the rather limited stability of the protein even with uncharged histidines, i.e., of the fairly low value of K_r. Expressed in terms of the standard free enthalpy, $\Delta G° = -RT \ln K_r$, we see that, irrespective of which model we choose, $\Delta G° \leq |5|$ kcal/mol at room temperature.

Saturation Transfer Experiments. In the experiments discussed in the preceding section no pH-dependent line broadening was detected for any of the histidine C2H resonances. Hence, the slow exchange process between the folded and unfolded form must be characterized by rate constants of about 1 s^{-1} or less. However, the equilibrium is established within a few minutes (see above) so the lifetimes of the folded and unfolded forms of E-L30 cannot be much longer than about 1 min.

In order to determine these lifetimes more accurately, magnetization transfer experiments were performed, the results of which are documented in Figure 7. The pH was adjusted so as to obtain approximately equal amounts of folded and unfolded protein (pH $\simeq$5.3). In the experiments the individual resonances of the histidine C2H protons were saturated by continuous irradiation during 1 s. The effect of this saturation on the other resonances was made visible by subtraction of two spectra: one in which a resonance was saturated and one in which preirradiation was performed in a part of the spectrum that contains no resonances. In the difference spectra thus obtained the dominant peak represents the irradiated resonance and small peaks represent saturation transfer (cf. Figure 7).

In Figure 7a it is seen that irradiation of the U1 resonance results in saturation transfer to the F1 resonance (belonging to His_{33}) and accordingly that irradiation of U2 gives rise to saturation transfer to F2 (His_{19}). Hence, the C2H proton of His_{33} resonates upfield from that of His_{19} in the random coil, and this situation is reversed in the folded form. Figure 7 also shows a rather puzzling effect, namely, that irradiation of the F resonances does not give rise to saturation transfer to the U resonances. Since the U and the F forms are about equally

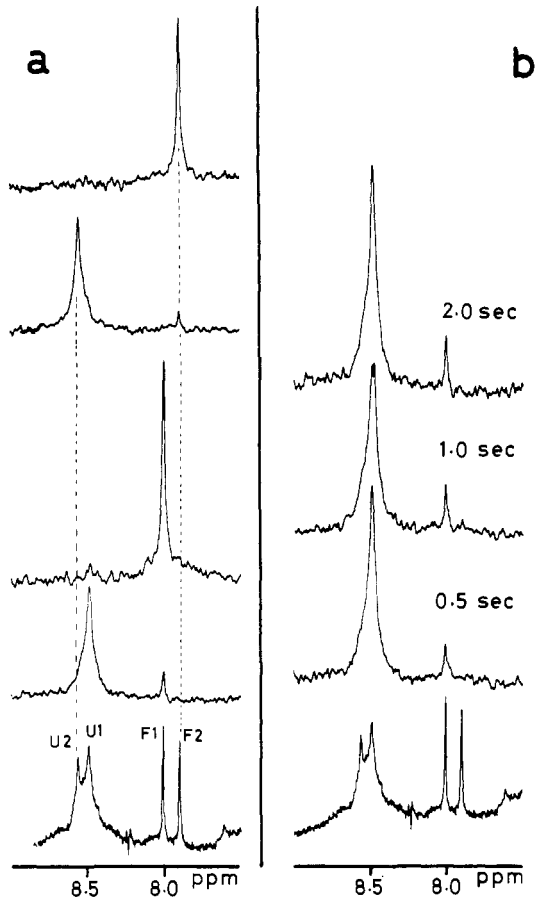

FIGURE 7: Difference spectra demonstrating the occurrence of magnetization transfer between the histine C2H resonances of folded and unfolded E-L30 protein. (a) Bottom trace is the unperturbed spectrum; the other traces represent difference spectra (see text) for which, proceeding from bottom to top, the resonances U1, F1, U2, and F2 had been presaturated, respectively. (b) Difference spectra exhibiting magnetization transfer after presaturation of resonance U1 for 0.5, 1.0, and 2.0 s in order to monitor the time dependence of the saturation transfer to F1.

abundant, they must have almost identical lifetimes, and one expects saturation transfer to be independent of direction, i.e., of equal magnitude when a U or a F resonance is irradiated. Since saturation transfer not only depends on the lifetimes of the species but also on rates of the spin–lattice relaxation, we are led to suspect a difference between the T_1 values of U and F resonances.

Indeed, a substantial difference between the longitudinal relaxation rates of U and F resonances was found (not shown). Spin–lattice relaxation times of C2H resonances of folded and unfolded E-L30 are in the order of magnitude of 1 and 0.1 s, respectively.

According to Figure 7b saturation transfer from U1 to F1 hardly increases when U1 is irradiated for 2 s instead of 1 s, suggesting that a steady-state situation is attained. In that case an estimation of the lifetime τ, which at this pH is equal for both folded and unfolded protein, may be obtained from the ratio r_{UF} of the intensities of the small (saturation transfer) and large (irradiated resonance) peaks of the difference spectrum shown in Figure 7b (top) according to

$$r_{UF} = (1 + \tau/T_1^F)^{-1} \qquad (7)$$

Here T_1^F is the longitudinal relaxation time of the F1 resonance ($T_1^F \simeq 1$s). We find that $r_{UF} = 0.14$ so that $\tau \simeq 7$ s.

This value of τ is in perfect agreement with the aforementioned observations: (i) no pH-dependent line broadening and

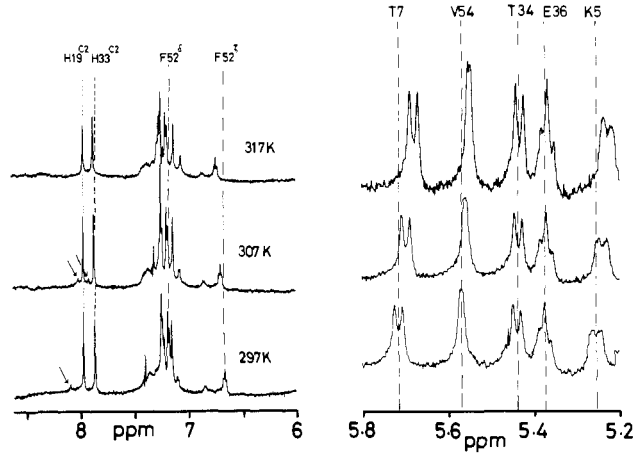

FIGURE 8: Temperature-dependent changes in the chemical shifts of some resonances in the 500-MHz ^{1}H NMR spectrum of protein E-L30. (Left) Temperature-dependent changes of the positions of the aromatic ring proton resonances. The arrows indicate the positions of the histidine C2H resonances, U1 and U2, belonging to the unfolded protein. (Right) Temperature-dependent changes of the positions of some C$^\alpha$H resonances from protons in the interior of the triple-stranded β-sheet in protein E-L30. The assignment of the resonances (van de Ven & Hilbers, 1986a,b) is indicated.

(ii) equilibrium settled within a few minutes. Substituting the longitudinal relaxation time of the U resonances, $T_1^U \simeq 0.1$ s, in eq 7 we obtain the ratio r_{FU} for saturation transfer from F to U. Since $\tau/T_1^U \simeq 70$, we have that $r_{FU} \simeq 0.014$. In words, saturation transfer from F to U is about 10 times less efficient than saturation transfer from U to F because spin–lattice relaxation is about 10 times as fast for U resonances compared with F resonances.

Temperature Dependence. In addition to the pH stability of protein E-L30, we investigated the thermal stability by recording ^{1}H NMR spectra at various temperatures. Also, the two-dimensional correlated spectra, recorded at different temperatures in the course of the resonance assignments reported elsewhere (van de Ven & Hilbers, 1986a,b) were searched for temperature-dependent resonances.

Some typical spectra of a temperature series, recorded at pH 6.85, are shown in Figure 8. Two resonances clearly exhibit temperature-dependent chemical shifts: Phe$_{52}$ (C$^\zeta$H) and Thr$_7$ (C$^\alpha$H). Other resonances are also temperature dependent but less outspoken: Phe$_{52}$ (C$^\delta$H, C$^\epsilon$H), His$_{33}$ (C2H), His$_{19}$ (C4H), Val$_{54}$ (C$^\alpha$H), and Lys$_5$ (C$^\alpha$H). In the 2D spectra (not shown) we detected temperature-dependent chemical shifts for the following resonances: Thr$_{22}$ (C$^\gamma$H$_3$), Ala$_{12}$ (C$^\beta$H$_3$), Ala$_{21}$ (C$^\alpha$H), Ala$_{49}$ (C$^\beta$H$_3$), and Val$_{54}$ (C$^\gamma$H$_3$). In Figure 6 the positions of all amino acids mentioned above have been indicated in the three-dimensional structure of E-L30.

Figure 6 clearly indicates clustering of residues with chemical shifts that are susceptible to pH and/or temperature, and it may be asked whether pH dependence and temperature dependence are caused by similar mechanisms. This question is addressed by comparing Figures 2 and 5 with Figure 8. It is seen that lowering pH and raising temperature have similar effects on a few resonances, i.e., Phe$_{52}$ (C$^\zeta$H) and Thr$_7$ (C$^\alpha$H), but the two phenomena are markedly different for other resonances; e.g., Thr$_{34}$ (C$^\alpha$H) is shifting more in Figure 5 than in Figure 8, and the reverse is found for Val$_{54}$ (C$^\alpha$H). Also, the C2H resonance of His$_{19}$ is temperature independent, and that of His$_{33}$ shows only a marginal effect compared with the shifting of this resonance as a function of pH (cf. Figures 2 and 8). We consider it therefore likely that lowering of pH has a different effect on the molecule than increasing the temperature. The pH-dependent shifting of resonances is most

likely merely reflecting titration of histidines whereas the temperature dependence of, the same, resonances is likely to be caused by a change in conformation which may well be as subtle as an increased amplitude of "breathing" of the molecule.

When the temperature was raised above 320 K, no changes in the spectrum were observed, apart from the shifting of resonances discussed above, but there was a rapid decrease in signal/noise ratio caused by precipitation of protein. This means that thermal denaturation involves an entirely different mechanism, compared with pH denaturation, attended with aggregation of protein.

In Figure 8 it is seen that the intensities of U resonances (arrows) do not change as a function of temperature, but their chemical shifts are strongly temperature dependent. In order to investigate whether the U/F equilibrium is influenced by temperature, we raised the temperature of the sample used for the saturation transfer experiments (vide supra) by 10 deg to 307 K and found no significant change in relative intensities of U and F resonances (not shown). We estimate that the maximal change in the fraction of folded protein, θ, that could give rise to an undetectable change in the intensity ratio of U and F peaks is about 10%. Hence, not detecting such a change means that a maximum value for the standard enthalpy of the pH-induced unfolding process may be derived, which is about 7 kcal/mole. Since this figure is in the same order of magnitude as the total free enthalpy for the folding of uncharged protein (vide supra), it is concluded that we just cannot measure θ accurately enough to assess the relative contributions of entropy and enthalpy to the stability of E-L30 in solution.

Conclusions

In this paper we have demonstrated that E-L30 reversibly unfolds with decreasing pH. This unfolding essentially takes place between pH 5.7 and pH 5.0. The steep relation between fraction of folded protein, θ, and pH can be explained if it is assumed that in addition to histidines His_{19} and His_{33} several other residues (Glu, Asp) have lower pK's in folded E-L30 compared with random coiled protein. This finding is in good agreement with the observation (van de Ven & Hilbers, 1986b) that the histidines are buried in a hydrophobic domain of the molecule (at least one of them involved in a hydrogen bond) and that Glu and Asp residues are involved in ion pairs. Since, glutamate is known as a strong "α-helix former" and as a "β-breaker" (Chou & Fasman, 1978; Cantor & Schimmel, 1980), the presence of all four Glu's of E-L30 in a triple-stranded β-sheet may be regarded as a destabilizing factor which is probably compensated for by the formation of these ion pairs. Protonation of histidines is likely to destabilize hydrophobic interactions in the interior of the molecule as well as the hydrogen bond between His_{33} and Arg_{29}, and protonation of Glu or Asp disrupts the ionic interactions of these residues with Arg or Lys side chains. The pH-dependent unfolding described in this paper for E-L30 is not observed for the 53% homologous, and structurally similar, protein B-L30 from *B. stearothermophilus* (J. Dijk, personal communication). In contrast to E-L30, the B-L30 molecule does not contain the two buried histidines; instead, there are two glutamines at positions 19 and 33 in this protein (Kimura, 1984). Thus, the absence of pH-dependent unfolding for B-L30 supports our conclusion that His_{19} and His_{33} are primarily responsible for this process of E-L30. It is interesting to note that three glutamates in the β-sheet of E-L30, viz., Glu_{36}, Glu_{38}, and Glu_{57}, have been substituted for Val, Asn, and Lys, respectively, in B-L30. Perhaps the better overall (thermal) stability of B-L30 finds its origin in these substitutions.

Even with deprotonated Glu, Asp, and his side chains, the stability of the E-L30 conformation is rather limited ($\Delta G° \leq |5|$ kcal/mol). At equilibrium the average lifetimes of folded and unfolded protein are $\leq$10 s.

The folded form of E-L30 appears to possess some degree of conformational freedom. Increasing temperature causes shifting of resonances belonging to amino acids that are all located in a certain domain of the molecule. Most of the temperature-dependent resonances are situated away from their "typical" (random coil) positions at low temperature and shift in the direction of their "typical" chemical shifts when temperature is raised. This suggests that the structure becomes "looser" at higher temperatures; e.g., the downfield shifts of resonances of $C^{\alpha}H$'s in β-strands are inversely proportional to the distance between the $C^{\alpha}H$ proton and a peptide bond carbonyl group of the partner strand (Pardi et al., 1983), in the case of E-L30, Thr_7-$C^{\alpha}H$---OC-His_{33} and Thr_{34}-$C^{\alpha}H$---OC-Ile_6. Hence, reduction of the downfield shift of Thr_7 $C^{\alpha}H$, and not Thr_{34} $C^{\alpha}H$, may be taken as an indication that the C-terminal end of β-strand 3–9 and the N-terminal end of β-strand 33–38 are moving apart (see Figure 6).

In addition to being temperature dependent, resonances of Thr_7, Thr_3, and Phe_{52} are also pH dependent. Since these residues are close to His_{19} and/or His_{33}, it cannot be ascertained whether these pH dependencies are caused by the increasing degree of protonation of histidines, a conformational change, or both. However, since protonation of histidines eventually gives rise to complete unfolding of the molecule, it is likely that an increasing degree of histidine protonation in "native" E-L30 is accompanied with a "loosening" of the structure, which would agree with the directions of the observed shifts: upfield for $C^{\alpha}H$'s of Thr_7 and Thr_{34} and downfield for $C^{\beta}H$ of Phe_{52}.

Figure 6 clearly shows residues affected by pH and/or temperature to be located in a particular site of the molecule. In fact, the somewhat elongated E-L30 molecule appears to consist of a "tight" end, constituted by the C-termini of the exterior β-strands, the N-terminus, and the greater part of α-helix 42–51, and a "loose" end, comprising the N-termini of the exterior β-strands, the C-terminus of the middle strand, the N-terminus of α-helix 20–26, and the "hinge" region between α-helix 42–51 and the C-terminal β-strand. It is quite likely that both large loops 27–31 and 10–17 also belong to the "loose" part of the molecule. Interestingly, in comparing the amino acid sequences of E-L30 and B-L30, the "loose" part of the molecule contains many more conserved residues than the "tight" part (van de Ven & Hilbers, 1986b).

If we examine the distribution of the charged residues in E-L30, lysines-2, -5, -18, -20, and -55, arginines-10, -15, -29, -30, -37, and -44, glutamates-36, -38, -57, and -58, and aspartate-39, some remarkable features are seen. First, all Glu and Asp residues are present in the antiparallel β-sheet, and together with three Lys (2, 5, 55) and Arg_{37} they constitute the solvent-exposed side of the sheet. Second, with the sole exception of Arg_{44}, the remaining ionized side chains are all positively charged and are all located in the "loose" end of the molecule (Figure 6). It is tempting to speculate that this "loose" end of E-L30 gains some extra stabilization in situ in the ribosome by ion–ion interactions.

Acknowledgments

J. Pompl and B. Delwig are acknowledged for their assistance during the pH titration experiments. M. Havekes isolated protein E-L30. The spectra were recorded at the Na-

tional Dutch 200/500 SON/ZWO hf NMR facility at Nijmegen. P. A. W. van Dael, W. Guijt, and C. A. G. Haasnoot are thanked for keeping the apparatus in excellent condition.

Registry No. His, 71-00-1.

REFERENCES

Appelt, K., Dijk, J., Reinhardt, R., Sanhuesa, S., White, S. A., Wilson, K., & Yonath, A. (1981) *J. Biol. Chem. 256*, 11787–11790.

Appelt, K., Dijk, J., White, S., Wilson, K., & Bartels, K. (1983) *FEBS Lett. 160*, 72–74.

Billiter, M., Braun, W., & Wüthrich, K. (1982) *J. Mol. Biol. 155*, 321–346.

Bundi, A., & Wüthrich, K. (1979) *Biopolymers 18*, 285–297.

Campbell, I. D., Dobson, C. M., & Rathcliffe, R. G. (1977) *J. Magn. Reson. 27*, 455–463.

Cantor, C. R., & Schimmel, P. R. (1980) Part I, p 49, Freeman, San Francisco.

Chou, P. Y., & Fasman, G. D. (1978) *Annu. Rev. Biochem. 53*, 251–276.

Giri, L., Franz, A., & Dijk, J. (1979) *Biochemistry 18*, 2520–2525.

Glickson, J. D., McDonald, C. C., & Phillips, W. D. (1969) *Biochem. Biophys. Res. Commun. 35*, 492–498.

Gudkov, A. T., Venyaminov, S. Yu., Behkle, J., & Bushuev, V. N. (1982) *FEBS Lett. 141*, 254–256.

Hartel, A. J., Lankhorst, P. P., & Altona, C. (1982) *Eur. J. Biochem. 129*, 343–357.

Jardetzky, O (1981) *Acc. Chem. Res. 14*, 291–298.

Kime, M. J., Ratcliffe, R. G., Moore, P. B., & Williams, R. P. J. (1981) *Eur. J. Biochem. 116*, 269–276.

Kimura, M. (1984) *J. Biol. Chem. 259*, 1051–1055.

Leyonmarck, M., Erikson, S., & Liljas, A. (1980) *Nature (London) 286*, 824–826.

Littlechild, J., Morrison, C. A., & Bradburry, E. (1979) *FEBS Lett. 104*, 90–94.

Matthew, J. B., Gard, F. R. N., Garcia-Moreno, B. E., Flanagan, M. A., March, K. L., & Shire, S. J. (1985) *Crit. Rev. Biochem. 18*, 91–197.

Moonen, C. T. W., & Müller, F. (1984) *Eur. J. Biochem. 140*, 303–309.

Nagayama, K., & Wüthrich, K. (1980) *Eur. J. Biochem. 114*, 365–374.

Ogawa, S., & Shulman, R. G. (1972) *J. Mol. Biol. 70*, 315–336.

Pardi, A., Wagner, G., & Wüthrich, K. (1983) *Eur. J. Biochem. 137*, 445–454.

Richarz, R., Sehr, P., Wagner, G., & Wüthrich, K. (1979) *J. Mol. Biol. 130*, 19–30.

Ritter, E., & Wittmann-Liebold, B. (1975) *FEBS Lett. 60*, 153–155.

Stark, G. R. (1967) *Methods Enzymol. 11*, 125–138.

Strop, P., Wider, G., & Uthrich, K. (1983) *J. Mol. Biol. 166*, 641–667.

Sudmeier, J. L., Evelhoch, J. L., & Johsson, N. B. H. (1980) *J. Magn. Reson. 40*, 377–390.

Tandord, C. (1968) *Adv. Protein Chem. 23*, 121–282.

van de Ven, F. J. M., & Hilbers, C. W. (1986a) *J. Mol. Biol. 192*, 389–417.

van de Ven, F. J. M., & Hilbers, C. W. (1986b) *J. Mol. Biol. 192*, 419–441.

van de Ven, F. J. M., de Bruin, S. H., & Hilbers, C. W. (1983) *Eur. J. Biochem. 134*, 429–438.

van de Ven, F. J. M., de Bruin, S. H., & Hilbers, C. W. (1984) *FEBS Lett. 169*, 107–111.

Wagner, G., & Wüthrich, K. (1979) *J. Mol. Biol. 130*, 31–37.

Wagner, G., Kumar, A., & Wüthrich, K. (1980) *Eur. J. Biochem. 114*, 375–384.

White, F. H. (1967) *Methods Enzymol. 11*, 481–484.

Williamson, M. P., Marion, D., & Wüthrich, K. (1984) *J. Mol. Biol. 173*, 341–359.

Wittmann, H. G. (1982) *Proc. R. Soc. London, B 216*, 117–135.

Wüthrich, K., Wider, G., Wagner, G., & Braun, W. (1982) *J. Mol. Biol. 155*, 311–319.

Wystop, G., Teraoka, H., Schulze, H., Hampl, H., & Nierhaus, K. H. (1979) *Eur. J. Biochem. 100*, 101–113.